Mutual Information between Input and Output Trajectories of Biochemical Networks

Filipe Tostevin and Pieter Rein ten Wolde

FOM Institute for Atomic and Molecular Physics, Kruislaan 407, 1098 SJ Amsterdam, The Netherlands
(Received 29 December 2008; published 27 May 2009)

Biochemical networks can respond to temporal characteristics of time-varying signals. To understand how reliably biochemical networks can transmit information we must consider how an input signal as a function of time—the input trajectory—can be mapped onto an output trajectory. Here we estimate the mutual information between input and output trajectories using a Gaussian model. We study how reliably the chemotaxis network of *E. coli* can transmit information on the ligand concentration to the flagellar motor, and find the input power spectrum that maximizes the information transmission rate.

Cells continually have to respond to a wide range of intra- and extracellular signals. These signals have to be detected, encoded, transmitted, and decoded by biochemical networks. In the absence of biochemical noise, a particular input signal will lead to a unique output signal, allowing the cell to respond appropriately. Recent experiments, however, have vividly demonstrated that biochemical networks can be highly stochastic [1], and a key question is therefore how reliably biochemical networks can transmit information in the presence of noise.

To address this question, we must recognize that the message may be contained in the temporal dynamics of the input signal. A well-known example is bacterial chemotaxis, where the concentration of the intracellular messenger protein depends not on the current ligand concentration, but rather on whether this concentration has changed in the recent past [2]—the response of the network thus depends on the *history* of the input signal. Moreover, the input signal may be encoded into the temporal dynamics of the signal transduction pathway. For example, stimulation of the rat PC-12 system with a neuronal growth factor gives rise to a sustained response of the Raf-Mek-Erk pathway, while stimulation with an epidermal growth factor leads to a transient response [3]. In all these cases, the message is encoded not in the concentration of some chemical species at a specific moment in time, but rather in its concentration as a function of time. Importantly, whether the processing network can reliably respond to a signal depends not only on the instantaneous value of the signal, but also on the time scale over which it changes. In general, the input and output signals of biochemical networks are time-continuous signals with nonzero correlation times. To understand how reliably biochemical networks can transmit information, we need to know how accurately an input signal as a function of time—the input trajectory—can be mapped onto an output trajectory. In this article, we take an information theoretic approach to this question.

A natural measure for the quality of information transmission is the mutual information between the input signal I and the network response O, given by $M(I, O) = H(O) - H(O|I)$ [4]. Here, $H(O) \equiv - \int dO\, p(O) \log p(O)$, with $p(O)$ the probability distribution of O, is the information entropy of the output O; $H(O|I) \equiv - \int dI\, p(I) \times \int dO\, p(O|I) \log p(O|I)$ is the average (over inputs I) information entropy of O given I, with $p(O|I)$ the conditional probability distribution of O given I. Recently, the mutual information between the instantaneous values of the input and output signals of biochemical networks has been investigated [5,6], although in these studies the temporal correlations in the input signals were ignored. Here we investigate the mutual information between input and output trajectories.

Mutual information between trajectories.—We consider a biochemical network in steady state which has one input species S with copy number S and one output species X with copy number X. The mutual information between input and output trajectories is found by taking the possible input and output signals I and O to be the possible trajectories $S(t)$ and $X(t)$:

$$M(S, X) = \int \mathcal{D}S(t) \int \mathcal{D}X(t)\, p(S(t), X(t))$$
$$\times \log \frac{p(S(t), X(t))}{p(S(t))p(X(t))}. \tag{1}$$

Calculating the mutual information between trajectories is in general a formidable task, given the high dimensionality of the trajectory space. However, for a Gaussian model, which we will employ here, the mutual information can be obtained analytically.

In this Gaussian model, it is assumed that the input signal consists of small temporal variations around some steady-state value, obeying Gaussian statistics. This limits our approach, but seems a reasonable simplification given that the input statistics have not been measured for most, if not all, biological systems. Moreover, we assume that the coupling between the components can be linearized and that the intrinsic noise is small and Gaussian, according to the linear-noise approximation [7]; recent modeling studies have shown this gives a good description of the noise properties of a large class of biochemical networks, even when the copy numbers are as low as ten [6,8]. Under these assumptions the joint probability distribution of the input

and output signals is described by a multivariate Gaussian,

$$p(\mathbf{v}) = \frac{1}{(2\pi)^N |\mathbf{Z}|^{1/2}} \exp\left(-\frac{1}{2}\mathbf{v}^T \mathbf{Z}^{-1}\mathbf{v}\right). \qquad (2)$$

The vector $\mathbf{v} \equiv (\mathbf{s}, \mathbf{x})$, with $\mathbf{s} = (s(t_1), s(t_2), \dots, s(t_N))$ constructed from the input signal sampled at times $t_1, \dots, t_N$, and $\mathbf{x} = (x(t_1), x(t_2), \dots, x(t_N))$; $s(t)$ and $x(t)$ are the deviations of S and X from their steady-state values, $\langle S \rangle$ and $\langle X \rangle$. The covariance matrix $\mathbf{Z}$ has the form

$$\mathbf{Z} = \begin{pmatrix} \mathbf{C}^{ss} & \mathbf{C}^{xs} \\ \mathbf{C}^{sx} & \mathbf{C}^{xx} \end{pmatrix}, \qquad (3)$$

where $\mathbf{C}^{\alpha\beta}$ is an $N \times N$ matrix with elements $\mathbf{C}^{\alpha\beta}_{ij} = C_{\alpha\beta}(t_i - t_j) = \langle \alpha(t_i)\beta(t_j)\rangle$. In the limit that the input and output signals are time continuous, the mutual information rate between the input and output trajectories $R(\mathbf{s}, \mathbf{x}) = \lim_{T\to\infty} M(\mathbf{s}, \mathbf{x})/T$ is given by [9]

$$R(\mathbf{s}, \mathbf{x}) = -\frac{1}{4\pi}\int_{-\infty}^{\infty} d\omega \ln\left[1 - \frac{|S_{sx}(\omega)|^2}{S_{ss}(\omega)S_{xx}(\omega)}\right], \qquad (4)$$

where the power spectrum $S_{\alpha\beta}(\omega)$ is the Fourier transform of $C_{\alpha\beta}(t)$. Measuring the output signal as a function of time, $R(\mathbf{s}, \mathbf{x})$ is the rate at which the information on the input trajectory increases with time; importantly, $R(\mathbf{s}, \mathbf{x})$ takes into account temporal correlations in the input and output signals. We emphasize that Eq. (4) is exact only for linear systems with Gaussian statistics. Importantly, however, Eq. (4) can also be applied to systems which do not obey Gaussian statistics and to nonlinear systems; in these cases it provides a lower bound on the channel capacity of the network [10].

A biochemical network differs from a channel in telecommunication or electronics, in that the reaction that detects the input signal may introduce correlations between the signal and the intrinsic noise of the reactions that constitute the processing network [8]; these correlations are a consequence of the molecular character of the components and thus unique to (bio)chemical systems. If the detection reaction does not introduce correlations, then the power spectrum of the output signal $S_{xx}(\omega)$ is given by the spectral addition rule [8]:

$$S_{xx}(\omega) = N(\omega) + g^2(\omega)S_{ss}(\omega). \qquad (5)$$

Here, $N(\omega)$ is the intrinsic noise of the processing network, $S_{ss}(\omega)$ is the power spectrum of the input signal, and $g^2(\omega) = |S_{sx}(\omega)|^2/S_{ss}(\omega)^2$ is the frequency-dependent gain. Identifying the spectrum of the transmitted signal as $P(\omega) = g^2(\omega)S_{ss}(\omega)$, Eq. (4) can be rewritten as

$$R(\mathbf{s}, \mathbf{x}) = \frac{1}{4\pi}\int_{-\infty}^{\infty} d\omega \ln\left[1 + \frac{P(\omega)}{N(\omega)}\right], \qquad (6)$$

a well-known result for a time-continuous Gaussian channel [11]. When the detection reaction does introduce correlations between the input signal and the noise of the processing network, one can still define $g^2(\omega)$ and $P(\omega)$ as above and apply Eq. (6). However, in this case $N(\omega)$ and $g^2(\omega)$ are not intrinsic properties of the network, but also depend on the statistics of the input signal.

Network motifs.—The three elementary detection motifs shown in Table I [8] illustrate a number of characteristics of the transmission of trajectories. As a simple example of a time-continuous input signal with a nonzero correlation time, we take the dynamics of S to be a Poissonian birth-and-death process; for large copy numbers, this gives distributions that are approximately Gaussian.

Motif I describes the reversible binding between, for example, a ligand and a receptor, or an enzyme and its substrate. For this motif only we take the input signal to be the total number of both bound and unbound molecules $S_T(t) = S(t) + X(t)$. We find that this motif acts as a low-pass filter for information. Specifically, the gain-to-noise ratio $g^2(\omega)/N(\omega)$, which determines how accurately an input signal at frequency ω can be transmitted, is approximately constant at low frequencies but decays as ω^{-2} for high frequencies. Since input signals of biochemical networks are commonly detected via this motif, this result suggests that high-frequency input signals are typically not propagated reliably.

Motif II describes the scenario in which the signaling molecule is deactivated upon detection. An important example is activation of membrane receptors by ligand binding followed by endocytosis. If the input signal is a Poissonian birth-and-death process, the mutual information between instantaneous values of s and x is zero [12]—x gives no information about the current value of s. Indeed, to understand how cells can use this motif to transmit information, we must consider the mutual information between input and output trajectories. Interestingly, for this motif $N(\omega)$ vanishes at high frequencies, while $g^2(\omega)$ approaches a constant value; the gain-to-noise ratio thus diverges at high frequencies, meaning that this motif can reliably transmit rapidly varying input signals [13].

Motif III is a coarse-grained model for enzymatic reactions or gene activation; the enzyme-substrate or transcription-factor-DNA binding reaction, respectively, has been integrated out. For this motif, which in contrast

TABLE I.   Three elementary detection motifs. The input signal is modeled via $\varnothing \xrightarrow{k} \mathsf{S}$ and $\mathsf{S} \xrightarrow{\lambda} \varnothing$.

Motif	Reaction	$g^2(\omega)$	$N(\omega)$	$\|S_{sx}(\omega)\|^2/S_{ss}(\omega)S_{xx}(\omega)$
(I)	$\mathsf{S} + \mathsf{W} \underset{\mu}{\overset{\nu=k_f W}{\rightleftharpoons}} \mathsf{X}$	$\left[\frac{\nu(\mu+\nu+\lambda)}{\omega^2+(\mu+\nu)^2+\nu\lambda}\right]^2$	$\frac{2\nu\langle S\rangle}{\omega^2+(\mu+\nu)^2+\nu\lambda}$	$\frac{\nu\lambda(\mu+\nu+\lambda)^2}{[\omega^2+(\mu+\nu)^2+\nu\lambda][\omega^2+\lambda(\lambda+\nu)]}$
(II)	$\mathsf{S} \xrightarrow{\nu} \mathsf{X} \xrightarrow{\mu} \varnothing$	$\frac{\nu^2[\omega^2+(\lambda+\nu)^2]}{4(\lambda+\nu)^2(\omega^2+\mu^2)}$	$\frac{\nu\langle S\rangle(4\lambda+3\nu)}{2(\lambda+\nu)(\omega^2+\mu^2)}$	$\frac{\nu}{4(\lambda+\nu)}$
(III)	$\mathsf{S} \xrightarrow{\nu} \mathsf{S} + \mathsf{X},\ \mathsf{X} \xrightarrow{\mu} \varnothing$	$\frac{\nu^2}{\omega^2+\mu^2}$	$\frac{2\nu\langle S\rangle}{\omega^2+\mu^2}$	$\frac{\nu\lambda}{\omega^2+\lambda(\lambda+\nu)}$

to the other two obeys the spectral addition rule [Eq. (5)], $g^2(\omega)$ and $N(\omega)$ have the same functional dependence on ω. Hence, $g^2(\omega)/N(\omega)$ is independent of ω, which means that this motif can transmit signals at all frequencies with the same fidelity.

For both motifs II and III the mutual information between trajectories does not depend on the deactivation rate μ of the readout component X; $g^2(\omega)$ and $N(\omega)$ depend in the same way on μ. The information on the input trajectory $s(t)$ is encoded solely in the statistics of the production events of X; decays of X occur independently of S and hence provide no new information about $s(t)$. These observations may suggest that if an input signal is detected via one of these motifs, the deactivation rate of X is not important. However, if the information encoded in $x(t)$ needs to be transmitted to a downstream pathway, then this transmission rate will in general depend on μ.

Bacterial chemotaxis.—A classical example of a biological system in which not only the instantaneous value of the input signal is important, but also its history, is the chemotaxis system of *Escherichia coli* [2]. The messenger protein CheY is phosphorylated (CheY$_p$) by the kinase CheA and dephosphorylated by the phosphatase CheZ. The kinase activity is rapidly inhibited by receptor-ligand binding, allowing the system to respond to changes in ligand concentration on short time scales. Receptor methylation slowly counteracts the effect of ligand binding on CheA activity, allowing the system to adapt to changes in ligand concentration on longer time scales. An open question is how this network processes the ligand signal in the presence of noise [14]. Here, we study how reliably the chemotaxis network can transmit information in time-varying input signals.

Recently, Tu *et al.* have shown that a minimal model can accurately describe the response of the chemotaxis system to a wide range of time-varying input signals [15]. In this model it is assumed that receptor-ligand binding and the kinase response are much faster than CheY$_p$ dephosphorylation and receptor (de)methylation; hence the kinase activity is in quasi-steady state. Linearizing around steady state, we obtain the following model [15]:

$$a(t) = \alpha m(t) - \beta l(t), \tag{7}$$

$$\frac{dm}{dt} = -\frac{a(t)}{\tau_m} + \eta_m(t), \tag{8}$$

$$\frac{dy}{dt} = \gamma a(t) - \frac{y(t)}{\tau_z} + \eta_y(t). \tag{9}$$

Here, $a(t)$ and $m(t)$ are, respectively, the deviations of the fraction of active kinases and the receptor methylation level from their steady-state values; $l(t)$ and $y(t)$ are the fractional changes in the ligand and CheY$_p$ concentrations relative to steady-state levels; τ_m and τ_z are the time scales for receptor (de)methylation and CheY$_p$ dephosphorylation, with $\tau_m > \tau_z$; η_m and η_y are Gaussian white-noise sources that are independent of one another, and of the

ligand signal: $\langle \eta(t) \rangle = 0$; $\langle \eta(t)\eta(t') \rangle = \langle \eta^2 \rangle \delta(t - t')$; $\langle \eta_m(t)\eta_y(t') \rangle = \langle \eta(t)l(t') \rangle = 0$. The statistics of the input signal are described by the power spectrum $S_{ll}(\omega)$. This system obeys the spectral addition rule [Eq. (5)], and the power spectrum of y is given by

$$S_{yy}(\omega) = N_{l\to y}(\omega) + g^2_{l\to y}(\omega)S_{ll}(\omega), \tag{10}$$

with $N_{l\to y}(\omega)$ and $g^2_{l\to y}(\omega)$ being intrinsic properties of the chemotaxis network:

$$g^2_{l\to y}(\omega) = \frac{\beta^2 \gamma^2 \omega^2}{(\omega^2 + \tau_z^{-2})(\omega^2 + \alpha^2/\tau_m^2)}, \tag{11}$$

$$N_{l\to y}(\omega) = \frac{\alpha^2 \gamma^2 \langle \eta_m^2 \rangle + (\alpha^2/\tau_m^2 + \omega^2)\langle \eta_y^2 \rangle}{(\omega^2 + \tau_z^{-2})(\omega^2 + \alpha^2/\tau_m^2)}. \tag{12}$$

Equation (11) shows that the gain is small at low frequencies, due to adaptation of the kinase activity via receptor methylation [15] [Fig. 1(a)]. This network is therefore unable to respond to low-frequency variations in the ligand signal. As noted in [15,16], the gain also decreases at high frequencies, due to the time taken for CheY$_p$ dephosphorylation by CheZ. However, we see that the noise also decreases with increasing frequency. In fact, at high frequencies the methylation dynamics can be ignored, and the dynamics of CheY$_p$ are approximately those of motif III, discussed above; $g^2_{l\to y}(\omega)/N_{l\to y}(\omega)$ increases to
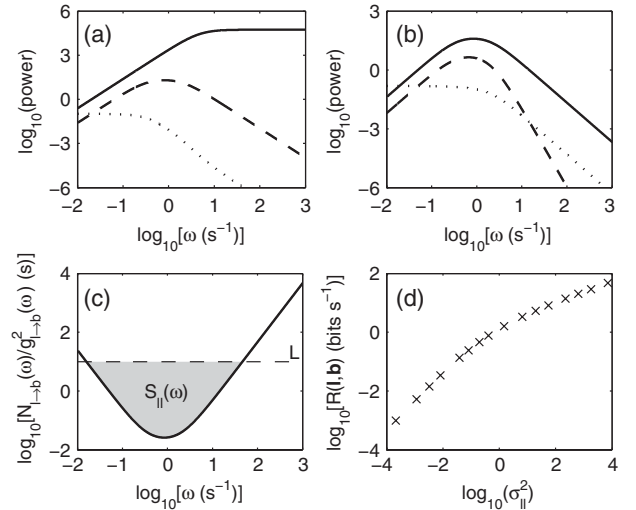

FIG. 1. Information transmission in the *E. coli* chemotaxis network. The network gain $g^2(\omega)$ (dashed line), noise $N(\omega)$ (dotted line), and $g^2(\omega)/N(\omega)$ (full line) are shown between (a) ligand and CheY$_p$ concentrations, and (b) ligand and motor bias. (c) Water filling approach for the optimal input signal [11]. The optimal power spectrum, subject to a total power constraint $\sigma^2_{ll} = \int_{-\infty}^{\infty} S_{ll}(\omega)d\omega$, is $S_{ll}(\omega) = L - N_{l\to b}(\omega)/g^2_{l\to b}(\omega)$, with L chosen such that the shaded area matches σ^2_{ll}. (d) $R(\mathbf{l}, \mathbf{b})$ evaluated numerically for different σ^2_{ll} values when the corresponding optimal input power spectrum is chosen. Parameter values were estimated from [15,16]: $\alpha = 2.7$, $\beta = 1.3$, $\tau_m = 8$ s, $\langle \eta_m^2 \rangle = 10^{-4}$ s^{-1}, $\gamma = 8$ s^{-1}, $\tau_z = 0.5$ s, $\langle \eta_y^2 \rangle = 0.002$ s^{-1}, $k = 1$ s^{-1}, $\tau_b = 0.5$ s, $\langle \eta_b^2 \rangle = 0.5$ s^{-1}.

a constant value showing that, in contrast to the conclusions of [15], high-frequency signals can be reliably encoded in the trajectory $y(t)$.

However, the ultimate response of this system is that of the flagellar motor. Binding of $CheY_p$ to the motor increases the tendency of the motor to switch to the clockwise state, which causes the bacterium to ''tumble'' and change direction. Assuming that $CheY_p$ binding to the motor is fast, and that the motor response can be linearized, the clockwise bias of the motor $b(t)$ is determined by

$$\frac{db}{dt} = ky(t) - \frac{b(t)}{\tau_b} + \eta_b(t), \qquad (13)$$

where τ_b is the typical motor switching time and η_b represents Gaussian white noise, uncorrelated from η_m and η_y. Applying Eq. (5), the power spectrum of the motor is $S_{bb}(\omega) = N_{y\to b}(\omega) + g^2_{y\to b}(\omega)S_{yy}(\omega)$, where $N_{y\to b}(\omega) = \langle \eta_b^2 \rangle/(\omega^2 + \tau_b^{-2})$ is the intrinsic noise of the motor, and $g^2_{y\to b}(\omega) = k^2/(\omega^2 + \tau_b^{-2})$ is the frequency-dependent gain of the motor. Inserting $S_{yy}(\omega)$ of Eq. (10), we see that the total noise added between the ligand and the motor is given by $N_{l\to b}(\omega) = N_{y\to b}(\omega) + g^2_{y\to b}(\omega)N_{l\to y}(\omega)$, while the overall gain of the network is $g^2_{l\to b}(\omega) = g^2_{l\to y}(\omega)g^2_{y\to b}(\omega)$.

Figure 1(b) shows that $g^2_{l\to b}(\omega)$ is large at frequencies $\tau_m^{-1} \lesssim \omega \lesssim \tau_z^{-1} \sim \tau_b^{-1}$, while $N_{l\to b}(\omega)$ monotonically decreases with increasing frequency. Importantly, at high frequencies $\omega \gg \tau_z^{-1}, \tau_b^{-1}$ the gain $g^2_{l\to b}(\omega) \sim \omega^{-4}$ since both $g^2_{l\to y}(\omega)$ and $g^2_{y\to b}(\omega)$ decrease as ω^{-2}, while $N_{l\to b}(\omega) \sim \omega^{-2}$ since the dominant noise contribution is the intrinsic noise of motor switching $N_{y\to b}(\omega)$; as a result, $g^2_{l\to b}(\omega)/N_{l\to b}(\omega)$ scales as ω^{-2}. Hence, while high-frequency fluctuations in $l(t)$ are reliably encoded in the trajectory $y(t)$, this information is not propagated to the motor. In essence, the high-frequency variations of $l(t)$ are filtered by the slow dynamics of $CheY_p$ dephosphorylation and motor switching, and are therefore masked by the inevitable intrinsic noise of motor switching.

The goal of the chemotaxis network is to determine whether the ligand concentration has increased or decreased. This binary decision has to be made on the time scale of a motor switching event, which means that the network should recover at least 1 bit of information from the input trajectory over this time scale: $R(\mathbf{l}, \mathbf{b}) > 1 \text{ bit}/\tau_b = 2 \text{ bits s}^{-1}$. Our results allow us to predict the input power spectrum $S_{ll}(\omega)$ that maximizes $R(\mathbf{l}, \mathbf{b})$ for a given power constraint σ_{ll}^2 [see Fig. 1(c)], which is peaked around $\omega \approx 1 \text{ s}^{-1}$. Figure 1(d) shows the corresponding optimal information rate as a function of σ_{ll}^2, and suggests that to achieve $R(\mathbf{l}, \mathbf{b}) > 2 \text{ bits s}^{-1}$ a signal variance of at least $\sigma_{ll}^2 \approx 2.5$ is required. The predicted form of the gain-to-noise ratio and the optimal input power spectrum could be tested by exposing *E. coli* cells to oscillating stimuli with different frequencies, for example in a microfluidic

device, and measuring the (cross) power spectra of the motor bias and the stimulus.

The input signal that a bacterium perceives depends not only on the spatiotemporal correlations of the ligand concentration in the environment but also on its swimming behavior, which in turn depends on the input signal itself: as Fig. 1(b) shows, *E. coli* is unable to reliably respond to high-frequency ($\omega \gg \tau_z^{-1}, \tau_b^{-1}$) or low-frequency ($\omega \ll \tau_m^{-1}$) stimuli. This means that, in order to find food, *E. coli* should swim neither too slowly nor too fast. Specifically, our predicted optimal input spectrum suggests that chemotaxis is most efficient when the spatiotemporal correlations of the ligand and the swimming speed of the bacterium are matched to give a typical frequency of the ligand signal of about $\omega \approx 1 \text{ s}^{-1}$. Further work is needed to study whether nature has optimized this feedback between swimming and signaling, and to explore the naturally occurring chemo-attractant distributions that *E. coli* would experience.

[1] M. B. Elowitz, A. J. Levine, E. D. Siggia, and P. S. Swain, Science **297**, 1183 (2002).

[2] S. M. Block, J. E. Segall, and H. C. Berg, J. Bacteriol. **154**, 312 (1983); J. E. Segall, S. M. Block, and H. C. Berg, Proc. Natl. Acad. Sci. U.S.A. **83**, 8987 (1986).

[3] C. J. Marshall, Cell **80**, 179 (1995).

[4] C. E. Shannon, Bell Syst. Tech. J. **27**, 379 (1948).

[5] P. B. Detwiler *et al.*, Biophys. J. **79**, 2801 (2000); G. Tkačik, C. G. Callan Jr., and W. Bialek, Proc. Natl. Acad. Sci. U.S.A. **105**, 12 265 (2008); Phys. Rev. E **78**, 011910 (2008).

[6] E. Ziv, I. Nemenman, and C. H. Wiggins, PLoS ONE **2**, e1077 (2007).

[7] N. G. Van Kampen, *Stochastic Processes in Physics and Chemistry* (North-Holland, Amsterdam, 1992).

[8] S. Tănase-Nicola, P. B. Warren, and P. R. ten Wolde, Phys. Rev. Lett. **97**, 068102 (2006).

[9] T. Munakata and M. Kamiyabu, Eur. Phys. J. B **53**, 239 (2006).

[10] P. P. Mitra and J. B. Stark, Nature (London) **411**, 1027 (2001).

[11] R. M. Fano, *Transmission of Information: A Statistical Theory of Communications* (MIT Press, Cambridge, MA, 1961).

[12] In the Gaussian model of Eq. (2), the mutual information between instantaneous values of s and x is $M^{\text{ins}}(s, x) = -\frac{1}{2}\ln[1 - \sigma_{sx}^4/(\sigma_{ss}^2\sigma_{xx}^2)]$, $\sigma_{\alpha\beta}^2 = \langle \alpha\beta \rangle$.

[13] $R(\mathbf{s}, \mathbf{x})$ for motif II diverges if the integral in Eq. (4) is taken to infinity. In reality the integral is bounded because a reaction cannot happen infinitely fast.

[14] B. W. Andrews, T.-M. Yi, and P. A. Iglesias, PLoS Comp. Biol. **2**, e154 (2006).

[15] Y. Tu, T. S. Shimizu, and H. C. Berg, Proc. Natl. Acad. Sci. U.S.A. **105**, 14 855 (2008).

[16] T. Emonet and P. Cluzel, Proc. Natl. Acad. Sci. U.S.A. **105**, 3304 (2008).